Erschienen in: Current Medicinal Chemistry ; 21 (2014), 3. - S. 365-376

The NOX1/4 Inhibitor GKT136901 as Selective and Direct Scavenger of Peroxynitrite

S. Schildknecht[1,*], A. Weber[1], H.R. Gerding[1], R. Pape[1], M. Robotta[2,5], M. Drescher[2,5], A. Marquardt[2], A. Daiber[3], B. Ferger[4] and M. Leist[1,5]

[1]In vitro Toxicology and Biomedicine, Department of Biology; [2]Department of Chemistry, University of Konstanz, 78457 Konstanz, Germany; [3]Molecular Cardiology, 2nd Medical Clinic, Medical Center of the Johannes Gutenberg University, Mainz, Germany; [4]CNS Diseases Research, Boehringer Ingelheim Pharma GmbH & Co. KG, 88397 Biberach an der Riss, Germany; [5]Konstanz Research School Chemical Biology, Kostanz, Germany

Abstract: NADPH oxidases (NOX), catalyzing the reduction of molecular oxygen to form the superoxide radical anion ($^{\bullet}O_2^-$) and hydrogen peroxide (H_2O_2), are involved in several pathological conditions, such as stroke, diabetes, atherosclerosis, but also in chronic neurodegenerative diseases such as Parkinson's disease, Alzheimer's disease, or multiple sclerosis. GKT136901 is a novel NOX 1/4 inhibitor with potential application in the areas of diabetic nephropathy, stroke, or neurodegeneration. In the present study, we investigated additional pharmacological activities of the compound with respect to direct free radical scavenging. GKT136901 did not interact with nitric oxide ($^{\bullet}NO$), $^{\bullet}O_2^-$, or hydroxyl radicals ($^{\bullet}OH$), but it acted as selective scavenger of peroxynitrite (PON) already in the submicromolar concentration range. Alpha synuclein (ASYN) is a protein involved in the pathogenesis of Parkinson's disease and a known target for PON dependent tyrosine nitration. Submicromolar concentrations of GKT136901 prevented tyrosine nitration and di tyrosine dependent dimer formation of ASYN by PON as indicated by Western blot and mass spectrometric analysis. GKT136901 itself was degraded when exposed to PON. In a human neuronal cell model, GKT136901 prevented both the depletion of reduced intracellular glutathione, and the degeneration of neurites when present during PON treatment of the cells. When GKT136901 was applied after PON treatment, no protective effect was observed, thus excluding an impact of GKT136901 on cellular death/survival pathways. In summary, selective scavenging of PON is an additional pharmacological property of the NOX 1/4 inhibitor GKT136901, and this may add to the efficiency of the drug in several disease models.

Keywords: Alpha synuclein, GKT136901, LUHMES, NADPH oxidase, NOX, peroxynitrite.

1. INTRODUCTION

NADPH oxidases (NOX) are a class of transmembrane multicomponent enzyme complexes that catalyze the transfer of an electron from NADPH to molecular oxygen to generate superoxide ($^{\bullet}O_2^-$) or hydrogen peroxide (H_2O_2) [1]. Enzymatic NOX activity was first identified in association with the phagocyte respiratory burst, a defence mechanism against pathogens [2, 3]. Enzyme complexes homologous to the phagocytic NOX have been subsequently identified in several different cell types and tissues [4, 5]. Today, the class of NOX enzymes comprises seven homologues. NOX-2 represents the originally discovered phagocytic NOX isoform [6, 7]. Other members are NOX-1, the human NOX-3, NOX-4, NOX-5, and the dual oxidases Duox-1 and Duox-2 [8-12]. Several NOX isoforms can serve as regulators of normal cell function by taking a role in the cellular redox regulatory system [13, 14]. Under pathophysiological conditions, such as hypoxia, diabetes, or inflammation, excessive and sustained activation of NOX can result in high fluxes of $^{\bullet}O_2^-$. The $^{\bullet}O_2^-$ ion alone, even at high concentrations, is usually not cytotoxic because of the presence of cytosolic and mitochondrial superoxide dismutases (Cu,Zn-SOD and Mn-SOD). Although it belongs to the oxygen radicals, $^{\bullet}O_2^-$ is only a weak oxidant and can even be regarded as reductant. High fluxes of $^{\bullet}O_2^-$ can represent a threat to cell viability, when nitric oxide ($^{\bullet}NO$), formed by one of three isoforms of nitric oxide synthase (NOS), is generated at a similar rate [15]. The radicals $^{\bullet}NO$ and $^{\bullet}O_2^-$ form peroxynitrite ($ONOO^-$) in an only diffusion-limited reaction [16, 17]. With a pK_a of 6.6, $ONOO^-$ exists in a cell partially in its protonated form peroxynitrous acid (ONOOH) that decomposes spontaneously into the highly reactive hydroxyl radical ($^{\bullet}OH$) and the nitrogen dioxide radical ($^{\bullet}NO_2$) [18, 19]. In contrast to $^{\bullet}O_2^-$ and $^{\bullet}NO$ alone, $^{\bullet}OH$ and $^{\bullet}NO_2$ represent highly reactive free radical species, capable of attacking proteins, lipids, and DNA. Nitration of tyrosine residues in proteins is predominantly mediated by the $^{\bullet}NO_2$ radical.

Selective inhibitors for the different NOS and NOX isoforms are expected to prevent oxidative damage under pathological conditions. While selective NOS-2 inhibitors such as AMT (2-Amino-5,6-dihydro-6-methyl-4H-1,3-thiazine) are

*Address correspondence to this author at the University of Konstanz; PO Box M657; 78457 Konstanz, Germany; Tel: +49 7531-88-5053; Fax: +49-7531-88-5039; E-mail: Stefan.Schildknecht@uni-konstanz.de

available, the development of NOX isoform-selective inhibitors is still in its infancy [20]. The peptide inhibitor Gp91phox ds-tat has a high selectivity for NOX-2 [21], but most of currently available NOX inhibitors display only little isoform selectivity and have a broad cross-reactivity. Diphenyleneiodonium (DPI), for example, is rather a general inhibitor of flavin-containing enzymes and inhibits also other enzymes such as NOS or xanthine oxidase [20]. The relatively new compound VAS2870 has been shown to inhibit not only NOX, but to interfere with signaling pathways that are involved in cell survival/cell death [22, 23]. The currently most widely used compound in basic research however is apocynin. It requires activation by peroxidases that are typically not sufficiently expressed in most cell types apart from leukocytes [24, 25]. Furthermore, apocynin is a direct scavenger of $^{\bullet}O_2^-$ and therefore acts as an $^{\bullet}O_2^-$ antioxidant rather than as an inhibitor of $^{\bullet}O_2^-$ generating NOX enzymes [26]. The pyrazolopyridine dione derivative GKT136901 has recently been identified as a selective NOX-1/NOX-4 inhibitor with a K_i of around 160 nM for NOX-1 and NOX-4 (human), compared with a K_i of 1500 nM for NOX-2 [23, 27]. Potential fields of application that involve NOX-1 are atherosclerosis, hypertension, inflammation, or cancer; NOX-4 is involved in idiopathic pulmonary fibrosis, chronic kidney diseases, or neurodegenerative diseases [28-32]. In the brain NOX-1 and -4 are expressed not only in microglia and astrocytes, but also in neurons [15, 33-36].

The NOX inhibitors currently used in basic research such as apocynin, or DPI, demonstrated significant off-target effects. For studies that investigate the mode of action of NOX inhibitors in disease models, it is necessary to distinguish between the direct effect of the compound on the respective enzyme activities, and the scavenging of oxidants that occurs independently from NOX inhibition. In the present study, we examined whether the interaction of the NOX-1/4 inhibitor GKT136901 [23, 27] with biologically important reactive oxygen species could be pharmacologically relevant for its mode of action. The compound was found to be a potent and selective scavenger of PON when present already in the submicromolar concentration range. This activity may explain some of GKT136901's effects in complex disease models and it needs to be taken into account as additional mode of action, independently from the drug's direct inhibition of NOX-1 and NOX-4.

2. MATERIALS AND METHODS

Materials: GKT136901 (2-(2-chlorophenyl)-4-methyl-5-(pyridin-2-ylmethyl)-1H-pyrazolo[4,3-c]pyridine-3,6(2H,5H)-dione) and VAS2870 (1,3-Benzoxazol-2-yl-3-benzyl-3H-[1,2,3]triazolo[4,5-d]pyrimidin-7-yl sulfide; CAS-no. 7224 56-31-7) were synthesized according to published protocols [23, 27]. Sin-1 (3-morpholino-sydnonimine) (peroxynitrite generator), and Spermine-NONOate (nitric oxide donor) were purchased from Cayman Chemicals (Ann Arbor, MI). Dihydrorhodamine 123 (DHR 123) and TEMPONE-H were from Molecular Probes (Carlsbad, CA), L-012 was from Wako (Neuss, Germany). Wildtype alpha synuclein (ASYN), ascorbic acid, uric acid, apocynin, Cu,Zn-superoxide dismutase (Cu,Zn-SOD), KO_2, and AAPH (2,2´-azobis[2-methyl-propionamidine] dihydrochloride, were from Sigma (St. Louis, MO). Sin-1 and Spermine-NONOate solutions were prepared freshly before each experiment. PON was from Merck (Darmstadt, Germany). Photometric determinations of PON stock concentrations were performed routinely (λ_{max}: 302 nm; ε: 1670 L mol^{-1} cm^{-1}). PON was diluted in 4.7% NaOH. When PON was used, an equal amount of equimolar HCl was added to the respective sample. In cell-free experiments, PON (in NaOH) and the corresponding volume of equimolar HCl were added carefully as separate droplets in the inner ring of a reaction tube, closed and vortexed instantaneously and rigorously.

Radical detection: The interaction between GKT136901 and PON was monitored by the oxidation of dihydrorhodamine 123 (DHR 123) (2 μM) or by the luminol-derivative L-012 (100 μM) in 10 mM potassium phosphate buffer, pH 7.4 containing desferoxamine (100 μM, to prevent Fenton-chemistry reactions). The radical generating systems were incubated with the test compounds for 3 min at 37°C before the radical detection dyes DHR 123 or L-012 were added and incubated for 15 min. Both dyes were chosen, since they are relatively selective for steady-state PON levels in the submicromolar range. DHR 123 fluorescence (λ_{ex}=485 nm/ λ_{em}=538 nm) as well as L-012 luminescence were detected in 96-well plates using a TECAN Infinite M200 reader. The interaction of GKT136901 with superoxide was assessed in a system composed of luminol (100 μM) and KO_2 (20 μM) as superoxide source in the presence and absence of 250 U/ml Cu,Zn-SOD. Values obtained with SOD were subtracted as background.

$^{\bullet}$NO-detection: Interaction between $^{\bullet}$NO and GKT 136901 was investigated by the use of the $^{\bullet}$NO-releasing compound Spermine-NONOate (10 μM) and an $^{\bullet}$NO-electrode (Ami NO-700, Innovative Instruments, Quee Brooks Court, FL) in 10 mM potassium phosphate buffer, pH 7.4. The electrode was calibrated every day with $NaNO_2$ standards in 0.1 M H_2SO_4 plus 100 μM potassium iodide. The current difference between baseline buffer signal and the peak following addition of $NaNO_2$ served for calibration of the instrument. Measurements were performed in stirred glass tubes at 37°C.

Hydroxyl ($^{\bullet}$OH) radical generation: 2-desoxyribose is a target for $^{\bullet}$OH, its degradation serves as measure for $^{\bullet}$OH generation. For optical detection, derivatization of 2-desoxyribose degradation products and thiobarbituric acid is catalyzed in the assay. Hydroxyl radicals were generated by a combination of ferrous iron (Fe^{2+}) and H_2O_2 and detected by measurement of the formation of chromogens (at 532 nm) that originate from the interaction of desoxyribose degradation products with thiobarbituric acid. 100 μl of a 150 mM NaCl solution (pH 7.4) were combined freshly with 50 μl of 0.7 mM EDTA, 50 μl of 0.5 mM Fe^{2+} and 100 μl of sample in water. Hydroxyl radical generation was then initiated by the addition of 50 μl 0.5 mM H_2O_2. The mixture was incubated with additional 100 μl of 5 mM 2-desoxyribose for 20 min at 37°C under gentle shaking. Then, 250 μl of 1% thiobarbituric acid (in 50 mM NaOH) and 250 μl of 2.8% trichloroacetic acid (in water) were added, vortexed thoroughly, shortly centrifuged to remove debris, and read at 532 nm.

HPLC analysis. Detection of GKT136901 was performed on a Kontron HPLC system (Goebel Analytik, Au/Hallertau, Germany) composed of a model 560 autosampler, a model 520 pump unit, and a model 535 diode array detector set at 260 nm. Separation was carried out on a C18 nucleosil column (125 x 4 mm; 5 µm particle size) from Macherey Nagel (Düren, Germany) at room temperature. The mobile phase for GKT136901 analysis consisted of acetonitrile : water : triethylamine: sulphuric acid (12.50 : 86.18: 1.04 : 0.28 v/v; pH 2.3). The mobile phase was degassed with an online vacuum degasser and delivered isocratically at a flow-rate of 1.0 ml/min at an average pressure of 120 bar. Data analysis was performed with Geminyx III software (Goebel Analytik).

Cell culture: LUHMES cells are conditionally immortalized human fetal ventral mesencephalic neuronal precursor cells that were obtained by clonal selection. Differentiated LUHMES cells show a clear dopaminergic phenotype which was described in detail previously [37, 38]. Cells were propagated in Advanced DMEM/F12 (Gibco/Invitrogen, Darmstadt, Germany), 1x N2 supplement (Invitrogen), 2 mM L-glutamine (Gibco), and 40 ng/ml recombinant bFGF (R+D Systems; Minneapolis, MN). The differentiation process was initiated by addition of differentiation medium consisting of advanced DMEM/F12, 1x N2 supplement, 2 mM L-glutamine, 1 mM dibutyryl-cAMP (Sigma), 1 µg/ml tetracycline (Sigma), and 2 ng/ml recombinant human GDNF (R+D Systems). After 2 days, cells were trypsinized and collected in Advanced DMEM/F12 medium. Cells were seeded onto 24-well plates at a density of 160.000 cells/cm^2. The differentiation process was continued for additional 4 days. For the Sin-1/ PON treatment experiments, differentiation medium was exchanged to Hank´s balanced salt solution (HBSS) 1 h prior to the experiment and for the decomposition period of 4 h for Sin-1 to avoid interference with ascorbic acid in the medium. Then, advanced DMEM/F12 without additions was added for the remaining incubation period of 20 h.

Immunocytochemistry and analysis of neurite degeneration: Cells were fixed with 4% paraformaldehyde for 20 min at RT, permeabilized with 0.2% Triton X-100, washed, and blocked with 1% BSA (Calbiochem, San Diego, CA) in PBS for 1 h. For visualization of cell morphology, cells were stained with a polyclonal anti-β-III-tubulin antibody (Covance, Munich, Germany; 1:1000) in 1% BSA/PBS at 4°C over night. After washing, the secondary antibody (anti-mouse-IgG, Alexa 488, Molecular Probes; 1:1000) in 1% BSA/PBS was added for 1 h, nuclei were stained by Hoechst dye H-33342 (1 µg/ml) for 20 min. For visualization, an Olympus IX 81 microscope (Hamburg, Germany) equipped with a F-view CCD camera was used. For quantitative evaluation of the neurite area, the β-III-tubulin-stained cells were analysed using an automated microplate-reading microscope (Array-Scan II® HCS Reader, Cellomics, Pittsburgh, PA) equipped with a Hamamatsu ORCA-ER camera (resolutuion 1024 x 1024; run at 2 x 2 binning) as previously described [39]. Briefly, nuclei were identified as objects according to their intensity, size, area and shape. A virtual area corresponding to the cell soma was defined around each nucleus. The total β-III-tubulin pixel area per field minus the soma areas in that field was defined as neurite mass.

Alpha synuclein nitration: Purified wildtype ASYN (Sigma) (10 µg/200 µl potassium phosphate buffer 100 mM, pH 7.4) was treated in the presence of various concentrations of test compounds with 1 µM PON. Five µl of PON (stock 1 mM in 4.7% NaOH) and 5 µl of 4.7% HCl were carefully placed in the inner lid of a reaction tube. After gentle closing, the samples were rapidly vortexed for optimal nitration at constant pH.

Western-blot: ASYN from the nitration experiments was loaded onto a 12% SDS gel (0.1 µg/lane). Proteins were transferred onto nitrocellulose membranes (Amersham, Buckinghamshire, UK), blocked with 5% milk in PBS-Tween (0.1%) for 2 h. Monoclonal antibodies directed against ASYN (1:1000) (BD, Frankin Lakes, NJ, USA) or against 3-nitrotyrosine (3-NT) (1:250) (HBT, HM5001, Uden, The Netherlands) were incubated at 4°C over night. The horseradish-peroxidase conjugated secondary antibody (Goat-anti-mouse IgG, Cyman Chemicals, Ann Arbor, MI, USA) was incubated for 45 min. For quantitative evaluation, luminescence was detected and quantified by a FUSION SL^{TM} system (Peqlab, Erlangen, Germany).

Resazurin metabolization assay: Resazurin (Sigma) was added to the cell culture medium in a final concentration of 2.5 µg/ml, fluorescence was measured in 15 min intervals (λ_{ex}=530 nm; λ_{em}=590 nm) over a period of 1 h.

Glutathione detection: Cells were washed twice with PBS and lysed in 200 µl of 1% sulfosalicylic acid (w/v) on ice. The lysates were collected, sonicated 3-4 times on ice and centrifuged at 12.000 x g for 5 min at 4°C to remove cell debris. Glutathione was determined by a DTNB (5,5´-dithiobis(2-nitrobenzoic acid)) reduction assay. Supernatants were diluted 1:10 in H_2O, 100 µl sample was mixed with 100 µl assay mixture containing 300 µM DTNB, 0.5 U/ml glutathione-reductase, 400 µM NADPH, 1 mM EDTA in 100 mM sodium phosphate buffer, pH 7.5 (all Sigma). DTNB reduction was measured photometrically at 405 nm in 5 min intervals over 30 min. Total protein content of each sample was detected after neutralization of the precipitated protein pellet with 100 mM NaOH by BCA reagent (Pierce, Thermo Scientific, Rockford, IL). GSH standard curves (Sigma) were performed by serial dilutions ranging from 1000 nM to 7.8 nM.

Electron paramagnetic resonance (EPR): measurements were performed at 20˚C using a MiniScope spectrometer (MS200, Magnettech GmbH) equipped with a variable temperature unit (Temperature Controller TC-H02, Magnettech GmbH). Samples were loaded into glass capillaries (outer diameter 1 mm) with typical sample volumes of 10 µl. Spectra were obtained in X-band (9.44 GHz) with a modulation amplitude of 0.6 G, microwave attenuation 10 dB and a sweep width of 100 G. The signal-to-noise ratio was improved by accumulation of 10 spectra featuring 60 s scan time each.

Mass spectrometric analysis: Alpha synuclein samples were analyzed by reversed phase liquid chromatography nanospray tandem mass spectrometry (LC-MS/MS) using an LTQ-Orbitrap mass spectrometer (Thermo Fisher) and an Eksigent nano-HPLC. The dimensions of the reversed-phase LC column were 5 µm, 200 Å pore size C18 resin in a 75 µm

i.d. × 10 cm long piece of fused silica capillary (Hypersil Gold C18, New Objective). After sample injection, the column was washed for 5 min with 95% mobile phase A (0.1% formic acid in water) and 5% mobile phase B (0.1% formic acid in acetonitrile), peptides were eluted using a linear gradient from 5 % mobile phase B to 40% mobile phase B within 65 min, then to 80% B within 5 min, at 300 nL/min. The LTQ-Orbitrap mass spectrometer was operated in a data dependent mode in which each full MS scan (30 000 resolving power) was followed by five MS/MS scans where the five most abundant molecular ions were dynamically selected and fragmented by collision-induced dissociation (CID) using a normalized collision energy of 35% in the LTQ ion trap. Dynamic exclusion was allowed. Tandem mass spectra were searched against the Swissprot human protein database using Mascot (Matrix Science) with "none" enzyme cleavage (because of the use of the unspecific protease pepsin), static cysteine alkylation by iodoacetamide, and variable nitration of Tyr and methionine oxidation.

All GKT136901 samples were analyzed by MS using an Esquire 3000 mass spectrometer (BrukerDaltonics) and an Agilent 1100 micro-HPLC, equipped with a Vydac MS C18 reversed phase column (Grace). After sample injection, the column was washed for 5 min with 90% mobile phase A (0.1% formic acid) and 10% mobile phase B (0.1% formic acid in acetonitrile). GKT136901 was eluted using 80% mobile phase B, with a flow rate of 50 µl/min. MS data were aquired in a mass range of m/z=200 to m/z=600.

Statistics: Values are expressed as the mean ± SD. If not otherwise indicated, experiments were performed at least three times with four technical replicates in each experiment. Data were analyzed by one-way ANOVA or Student´s t-test as appropriate, differences were determined by Bonferroni´s post hoc test (Prism or Origin software). If not otherwise indicated, means were considered as statistically significant at $p < 0.05$.

3. RESULTS

Scavenging of peroxynitrite-derived free radicals but not nitric oxide by GKT136901. Under physiological conditions, peroxynitrite ($ONOO^-$) partially exists in its protonated form peroxynitrous acid (ONOOH) that undergoes cleavage into the hydroxyl radical ($^{\bullet}OH$) and the $^{\bullet}NO_2$ radical, which is the principal nitrating agent. To investigate a potential novel pharmacological activity of GKT136901 as antioxidant, in addition to its direct action as NOX1/4 inhibitor, we tested its scavenging properties of PON-derived free radicals. The assay was based on the oxidation of DHR123 to rhodamine by the PON-generating compound Sin-1 that has a $t_{1/2}$ of ~ 45 min in the buffer used. PON generated under these conditions has a $t_{1/2}$ of ~ 1-2 s, so that a steady-state PON level of roughly 0.01% of the applied Sin-1 concentration is generated. Oxidation of DHR123 was significantly slowed by the presence of 0.1 µM GKT136901 and almost completely prevented by 10 µM GKT136901 (Fig. **1A**). Interaction of GKT136901 with $^{\bullet}NO$ was investigated with the help of a $^{\bullet}NO$-selective electrode. To ensure selective detection of $^{\bullet}NO$, the electrode was tested for potential responses to PON, $^{\bullet}O_2^-$, or hydroxyl radicals ($^{\bullet}OH$). In all these cases, no significant output was detected (not shown). As a source of $^{\bullet}NO$, the $^{\bullet}NO$ generating compound Spermine-NONOate was selected. Spermine-NONOate has a $t_{1/2}$ of ~ 45 min under the buffer conditions of the assay, and it releases 2 moles of $^{\bullet}NO$ per mol Spermine-NONOate. The fluxes of free $^{\bullet}NO$ were not significantly affected by the presence of GKT136901. A direct interaction of $^{\bullet}NO$ with GKT136901 does therefore not appear to play a pharmacological role in biological models (Fig. **1B**). In order to investigate the relevance of these findings in a cell system, human dopaminergic neurons (LUHMES) were treated either with Sin-1 or Spermine-NONOate for 6 h in the presence of varying concentrations of GKT136901. The levels of reduced glutathione (GSH) in the neurons were chosen as intracellular readout. GSH can be oxidized by PON into its oxidized GSSG form. Treatment of cells with an $^{\bullet}NO$-donor in the presence of oxygen can result in GSH depletion and the formation of nitrosoglutathione (GSNO). GKT136901 concentration-dependently prevented the drop in GSH evoked by Sin-1, but had no effect on the Spermine-NONOate dependent depletion of intracellular GSH levels (Fig. **1C**). The data indicate that GKT136901, next to its role as NOX-1/4 inhibitor, serves as selective scavenger of PON, respectively the $^{\bullet}NO_2$ radical, in biological systems. In the present study, LUHMES cells were used as neuronal model. The protective effect of GKT136901 in this model may in theory be due to the drug's peroxynitrite scavenging properties, or due to its role as inhibitor of NOX. To distinguish between these two mechanisms, we measured the expression of NOX family members on the mRNA level and NOX activity by radical detection in the LUHMES cells exposed to various conditions of cell activation. We did not detect any significant NOX activity or mRNA expression (not shown). Therefore, in all experiments including LUHMES and GKT136901, a significant contribution of NOX enzyme inhibition to the effects observed can be excluded.

Selective scavenging of PON by GKT136901. The scavenging capacity of GKT136901 on PON-derived radicals was directly compared in the Sin-1/DHR123 system with the best-known $^{\bullet}NO_2$-scavenger uric acid and with another NOX inhibitor, VAS2870. While VAS2870 was inactive at concentrations up to 100 µM, GKT136901 appeared even more efficient in scavenging PON-derived free radicals than uric acid (Fig. **2A**). To confirm our finding in a different test system, L-012 was chosen as alternative radical detection dye. Both GKT136901 as well as uric acid were even slightly more efficient in preventing L-012 oxidation, compared with DHR123 oxidation (Fig. **2B**). The observed difference between the two dyes is most likely based on their different interaction with peroxynitrite, or, more exactly, with its radical dissociation products. Under physiological buffer conditions, peroxynitrite partially exists in its protonated form peroxynitrous acid (ONOOH) that decomposes into the nitrogen dioxide ($^{\bullet}NO_2$) radical and the hydroxyl radical ($^{\bullet}OH$) [40]. Both radical species interact with DHR 123 and L-012. The respective contribution of $^{\bullet}NO_2$ or $^{\bullet}OH$ to DHR 123 or L-012 oxidation is not known, but most likely it is not identical. This would explain the variations in the curves obtained with DHR 123 or L-012 (Fig. **2A** & **B**). As the widely used NADPH oxidase inhibitors apocynin and DPI have been reported to exert significant off-target effects, they were also tested for their PON-scavenging properties. Ascorbic acid,

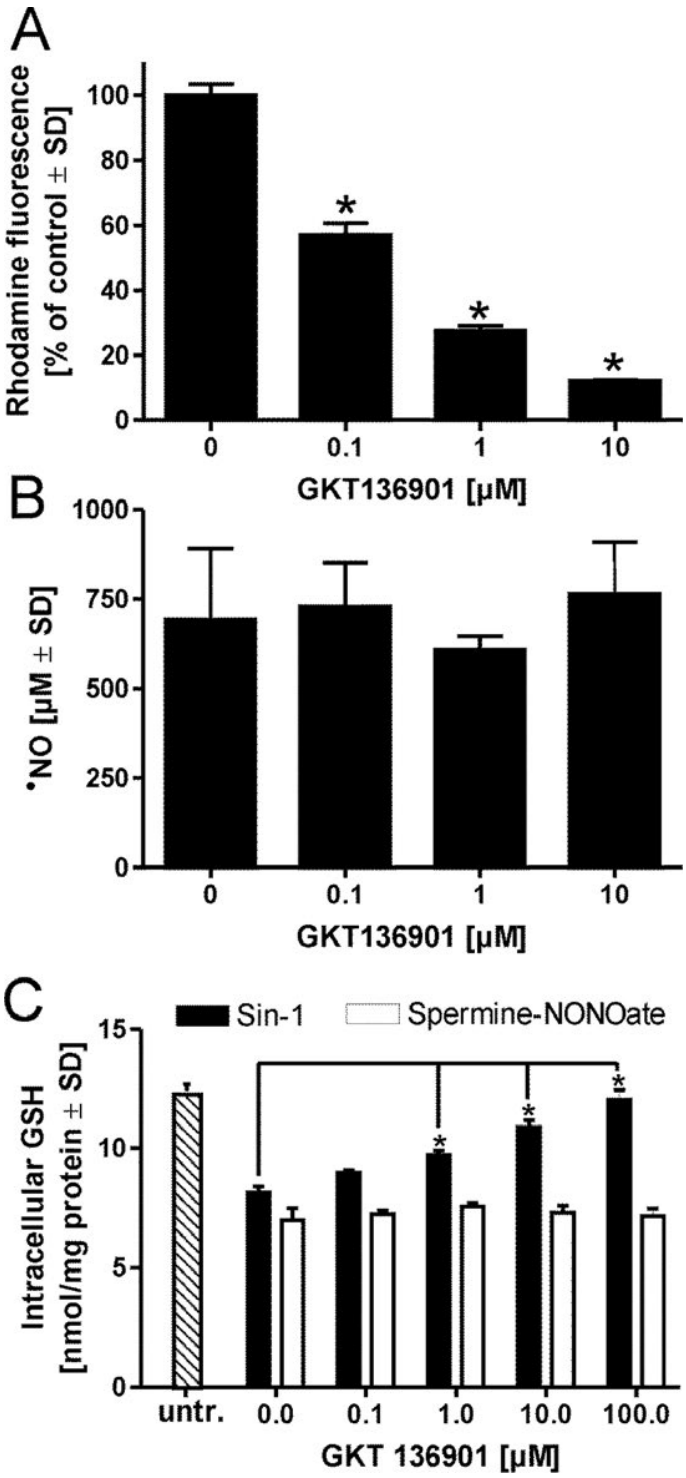

Fig. (1). Interaction of GKT136901 with peroxynitrite or nitric oxide. (**A**) GKT136901 was preincubated with the peroxynitrite generating compound Sin 1 (50 µM) for 3 min, followed by dihydrorhodamine 123 (DHR 123) (2 µM), and incubated for additional 15 min at 37°C. Upon oxidation of DHR 123, fluorescent rhodamine is generated. (**B**) To investigate the interaction of GKT136901 with nitric oxide (•NO), the •NO donor Spermine NONOate (10 µM) was added to GKT136901 present in the concentrations as indicated. Nitric oxide was measured by a •NO selective electrode over a period of 120 s. (**C**) Human dopaminergic neurons (LUHMES) were treated with GKT136901 in the concentrations as indicated for 15 min. Then, the peroxynitrite generating compound Sin 1 (500 µM) or the •NO generating compound Spermine NONOate (250 µM) were added for 6 h, levels of reduced glutathione (GSH) were detected in cell homogenates. The data are the means ± S.D. of three independent experiments with four technical replicates respectively. The statistical significance was determined by one way ANOVA, followed by Bonferroni's post hoc test. $^{*}p < 0.05$ versus PON.

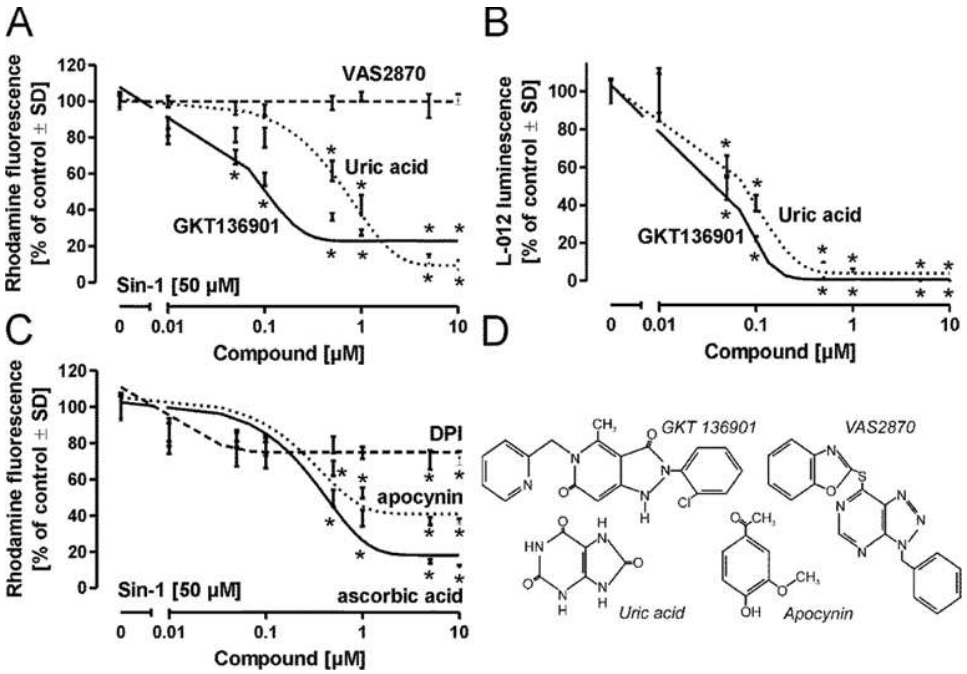

Fig. (2). GKT136901 as scavenger of peroxynitrite. GKT136901, VAS2870, DPI, apocynin, ascorbic acid, or the peroxynitrite scavenger uric acid, present in the concentrations indicated, were treated with the peroxynitrite generating compound Sin 1 (50 µM) for 3 min, followed by the addition of (**A**) + (**C**) DHR 123 (2 µM), or (**B**) L 012 (100 µM) and incubated for additional 15 min. Fluorescence of rhodamine, respectively luminescence of L 012 were detected. (**D**) Molecular structures of GKT136901, VAS2870, apocynin, and uric acid. The data are the means ± S.D. of four independent experiments with eight technical replicates respectively. The graphs illustrate sigmoidal dose response curves obtained by the equation y=Max+(Max Min)/(1+10^((logEC_{50} x)*Hill slope)). Rectangular hyperbola were obtained by nonlinear regression, y=Max*x/K_d+x. The statistical significance was determined by one way ANOVA, followed by Bonferroni's post hoc test. $^{*}p <$ 0.05 versus PON.

as a general antioxidant, served as positive control. Significant inhibition of DHR123 oxidation was observed with apocynin concentrations > 1 µM (Fig. **2C**). Together with a previous report on the $^{\bullet}O_2^-$ scavenging properties of apocynin [26], these data indicate that apocynin, in contrast to GKT136901, must rather be considered as a relatively unselective scavenger of free radical species. PON scavenging by apocynin was observed at ~ 10 fold higher concentrations compared with GKT136901 (Fig. **2C**). With respect to the structures, the scavenging of free radicals, especially $^{\bullet}NO_2$-radicals by uric acid was investigated in detail by Beckman and coworkers and may be explained by the formation of the triuret intermediate [41]. Apocynin contains an activated aromatic ring system with a phenolic $^{\bullet}OH$- and a methoxy group (both are +M ligands) explaining the potent free radical scavenging activity of this compound. Interestingly, neither the structures of GKT136901 nor VAS2870 contain classical antioxidant moieties and therefore provide no explanation for the observed differences in the antioxidant, free radical scavenging properties of these compounds. Only one tertiary and one secondary amine in GKT along with the cyclic amido-group (as in uric acid) may confer some antioxidant activity (Fig. **2D**).

To further explore the selectivity of the interaction of GKT136901 with PON, the scavenging properties towards authentic PON, $^{\bullet}O_2^-$, and hydroxyl radicals ($^{\bullet}OH$) were compared. As independent test system for the interaction with PON, EPR spectroscopy was applied to follow formation of the stable TEMPONE radical, originating from the interaction of TEMPONE-H with PON. GKT136901 and uric acid almost completely prevented TEMPONE formation. In contrast to that, the NOX inhibitor VAS2870 was inactive in this assay (Fig. **3A**).

A potential interaction of GKT136901 with superoxide ($^{\bullet}O_2^-$) was investigated by incubation with KO_2 and using luminol as detecting reagent. To ensure selectivity of the test for $^{\bullet}O_2^-$, all experiments were performed in parallel in the presence of superoxide dismutase (SOD), ascorbic acid was used as positive control. GKT136901 did not show any effect on KO_2-dependent luminol oxidation in the pharmacologically relevant concentration range (Fig. **3B**).

Interaction of GKT136901 with $^{\bullet}OH$ radicals was investigated in a system composed of Fe^{2+} and H_2O_2 as $^{\bullet}OH$ generating components and 2-desoxyribose as $^{\bullet}OH$-target. After treatment, 2-desoxyribose levels were detected by derivatization with thiobarbituric acid and optical detection. DMSO, as a known efficient scavenger of $^{\bullet}OH$, served as positive control. Neither GKT136901, nor VAS2870 displayed significant interaction with $^{\bullet}OH$ (Fig. **3C**). These observations indicate a selective interaction of GKT136901 with PON, respectively $^{\bullet}NO_2$, but not with other biologically relevant reactive oxygen- or nitrogen species.

Decomposition of GKT136901 by PON. We addressed the question whether GKT136901 would possibly be chemically modified under conditions associated with the production of PON. The compound was treated with increasing concentrations of PON and quantified before and after the

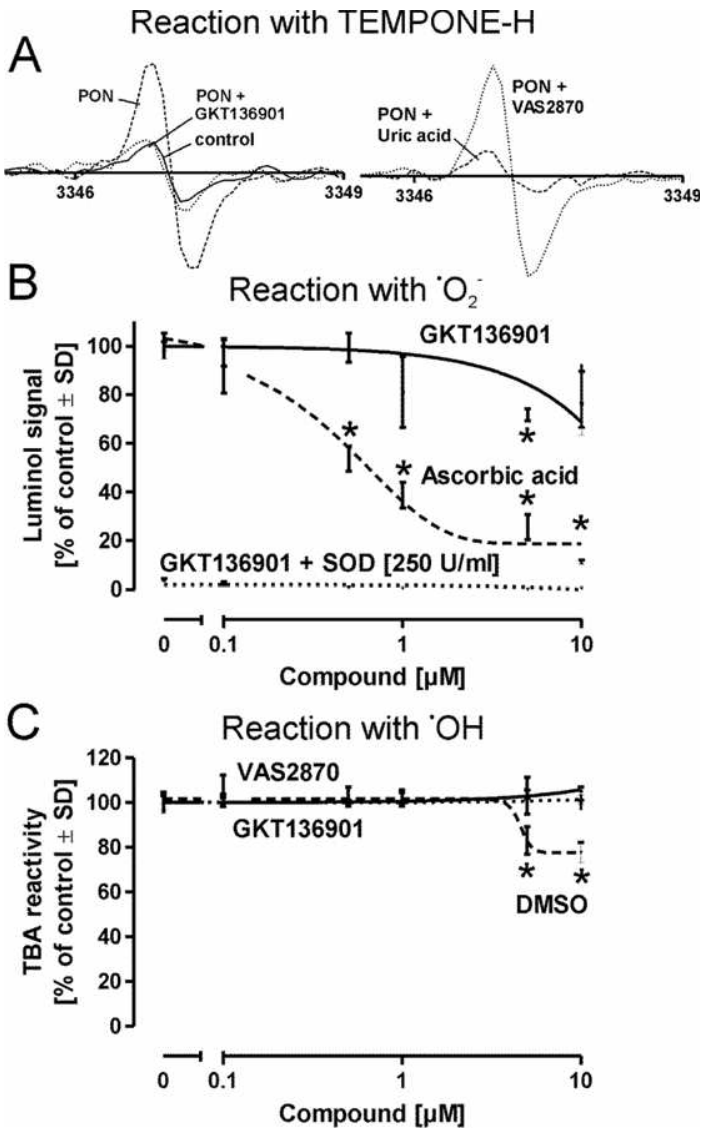

Fig. (3). Interaction of GKT136901 with different radical species. (**A**) EPR spectra monitoring the interaction of GKT136901 with per oxynitrite. The spin trap TEMPONE H (100 µM) was treated with authentic peroxynitrite (PON, 5µM), in the presence of GKT136901 (5 µM), VAS2870 (5 µM), or uric acid (50 µM). The stable TEMPONE radical was detected by EPR spectroscopy. The graphs are representa tive of three different experiments. The control shows the background signal of TEMPONE H without PON treatment. (**B**) Interaction of GKT136901 with superoxide ($^{\bullet}O_2^-$). GKT136901 or ascorbic acid were treated with KO_2 (20 µM). Luminol (100 µM) served as $^{\bullet}O_2^-$ detection dye. To exclude an involvement of other free radical species, GKT136901 was co incubated with superoxide dismutase (SOD, 250 U/ml). (**C**) Interaction of GKT136901 with hydroxyl radicals ($^{\bullet}OH$). GKT136901, VAS2870, or the $^{\bullet}OH$ scavenger DMSO were incubated with an $^{\bullet}OH$ generating system consisting of Fe^{2+} (50 µM) and H_2O_2 (50 µM). Degradation of 2 desoxyribose by $^{\bullet}OH$ was photometrically detected by derivatization with thiobarbituric acid (TBA). The data are the means ± S.D. of three independent experiments with four technical replicates respectively. The graphs illustrate sigmoidal dose response curves obtained by the equation y=Max+(Max Min)/(1+10^((logEC_{50} x)*Hill slope)). Rectangular hyperbola were obtained by nonlinear regression, y=Max*x/K_d+x. The statistical significance was determined by one way ANOVA, followed by Bonferroni's post hoc test. $^{*}p < 0.05$ versus PON.

reaction by HPLC analysis. The results suggest that GKT136901 was destroyed by the reaction with PON (Fig. **4A**). To compare the stability of the drug towards other reactive oxygen species, GKT136901 was treated with Sin-1, authentic PON, KO_2, or the $^{\bullet}OH$-generating compound AAPH. HPLC analysis showed that the amount of GKT136901 was reduced by roughly 20% by incubation with AAPH or KO_2. Treatment with PON lead to an almost complete disintegration of GKT136901 (Fig. **4B**). Samples of PON-treated GKT136901 were furthermore examined by mass spectrometry. The results confirmed the disappearance of the GKT136901 peak (*m/z* 367 Da) and suggested the generation of degradation products of GKT136901 as results of a complex disintegration (Fig. **4C**). We next tested whether the reaction products still had PON-scavenging properties. GKT136901, in a first experimental step, was treated with authentic PON or KO_2. Following this reaction and the decomposition of the oxidant, the resulting mixtures

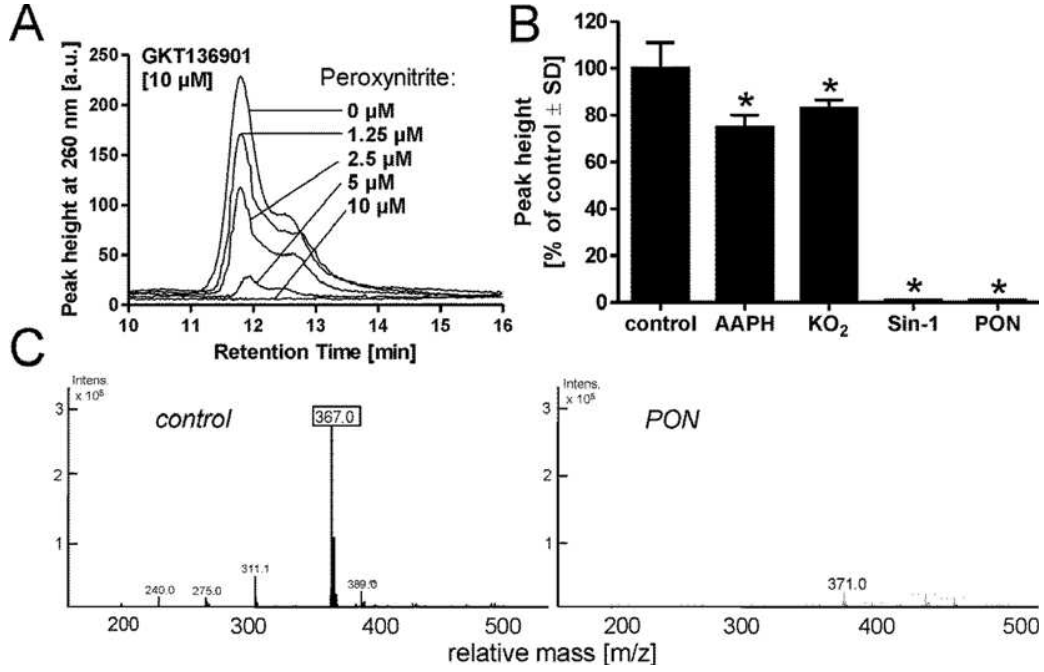

Fig. (4). Decomposition of GKT136901 by treatment with peroxynitrite. (**A**) GKT136901 (10 µM) was treated with various concentra tions of peroxynitrite and then quantified by HPLC analysis. (**B**) GKT136901 was treated with the hydroxyl radical generator AAPH (100 µM), KO_2 (10 µM) as a source of superoxide, the peroxynitrite generating compound Sin 1 (100 µM), or with authentic peroxynitrite (10 µM) for 24 h, GKT136901 was then quantified by HPLC analysis. (**C**) GKT136901 (10 µM) before and after treatment with 10 µM of authentic PON was analyzed by LC MS/MS mass spectrometry. The experiments were performed three times independently.

were added to the Sin-1/DHR123 detection system. GKT136901 that was not treated with PON before showed an inhibition of the Sin-1-dependent oxidation of DHR123 as expected. However, pretreatment with PON resulted in a concentration-dependent loss of GKT136901's ability to prevent Sin-1-mediated DHR123 oxidation (Fig. **5A**). Preincubation of GKT136901 with KO_2 did not affect the compound's ability to prevent DHR123 oxidation by Sin-1 (Fig. **5B**). As a control, VAS2870 was tested. It inhibited Sin-1 dependent oxidation of DHR123 only to a minor extent, no matter whether it was pretreated with PON or not (Fig. **5C**). Thus, it appears that GKT136901 is selectively destroyed by PON and that the degradation products do not show antioxidative reactivity.

Prevention of alpha synuclein (ASYN) nitration by GKT136901. ASYN is a key component in the pathogenesis of Parkinson's disease (PD) and a known target for several posttranslational modifications. The protein contains 4 tyrosine residues, its tyrosine-nitration has been shown both *in vitro* as well as *in vivo* in post mortem brain samples of human PD patients. As ASYN is also one of the most abundant brain proteins, it was chosen as a disease-relevant target for PON-mediated nitrations. The protein was treated with PON in the presence of varying concentrations of GKT136901 or VAS2870. Uric acid served as positive control. GKT136901 concentration-dependently prevented the nitration (3-NT) of the ASYN monomer (Fig. **6A**). Exposure of ASYN to PON also resulted in the formation of a protein band with a molecular mass of two ASYN monomers, indicating a covalent dimer formation, potentially via di-tyrosine formation. The formation of ASYN dimers was prevented by GKT136901 (Fig. **6A**). The presence of VAS2870 affected nitration or dimer formation by PON only marginally. To obtain more detailed information on the tyrosine residues actually nitrated under the experimental conditions employed, ASYN was treated with 5 µM PON in the presence and absence of 5 µM GKT136901 and analyzed by LC-MS/MS mass spectrometry. Similar to our previous observations, tyrosine residues Tyr^{125}, Tyr^{133}, and Tyr^{136}, but not Tyr^{39}, were nitrated by PON. GKT136901 prevented the nitration of all three tyrosine residues. (Fig. **6B**) provides a schematic summary of mass spectrometry data.

Protection of human neuronal cells from PON by GKT136901. The protection of cells from PON-toxicity by GKT136901 was finally tested in a cell culture model of human dopaminergic neurons (LUHMES) (Fig. **7A**). LUHMES cells possess no significant NOX activity, hence the influence of GKT136901 must be due to its peroxynitrite scavenging properties alone. For a quantitative assessment, neurite mass was detected with an automated microscope system, general cell viability was detected with the resazurin reduction assay (Fig. **7B**). PON treatment alone lead to severe damage of neurite integrity and ultimately lead to cell death. In one set of experiments, GKT136901 was added 5 min before the cells were treated with authentic PON (GKT136901 → PON) to study the compound's PON scavenging properties. A second set of experiments was performed to exclude that GKT136901 may have protected the cells due to an inhibition of death signaling cascades. In this set, cells were treated with PON first, and then, a few

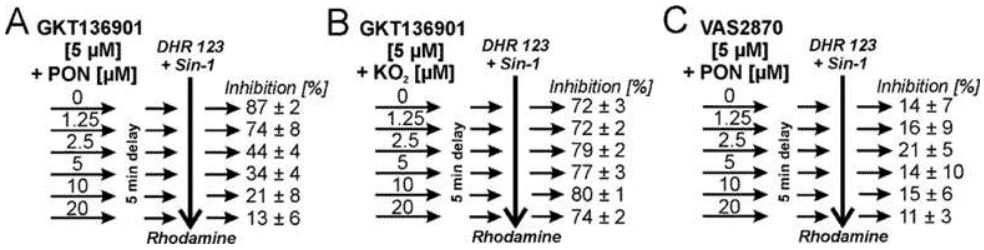

Fig. (5). PON pretreated GKT136901 loses its PON scavenging properties. GKT136901 (5 µM) or VAS2870 (5 µM) in a first step were treated with various concentrations of peroxynitrite (PON), or with KO_2. PON and KO_2 have a half life time in the range of seconds in aque ous solutions of neutral pH. After 5 min, the PON and KO_2 treated GKT136901/VAS2870 samples were exposed to the peroxynitrite generating compound Sin 1 (50 µM) and DHR 123 (2 µM) as radical detection dye. The capacity of pre treated GKT136901/VAS2870 to inhibit Sin 1 mediated DHR123 oxidation was detected. The data are the means ± S.D. of three independent experiments with four technical replicates respectively. The statistical significance was determined by one way ANOVA, followed by Bonferroni's post hoc test. $^{*}p < 0.05$ versus PON.

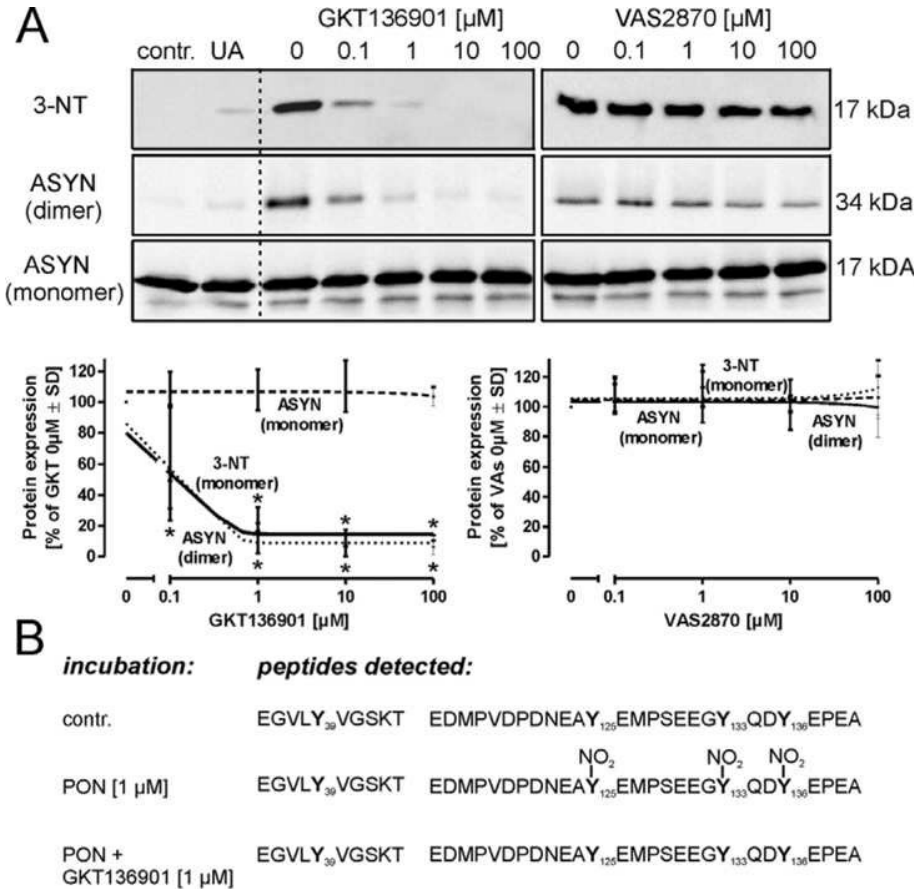

Fig. (6). GKT136901 prevents the nitration and dimer formation of alpha synuclein (ASYN). (**A**) Human recombinant ASYN (10 µg/200 µl) was nitrated by authentic peroxynitrite (1 µM) in the presence of GKT136901 or VAS2870. Control samples received no per oxynitrite, uric acid (UA, 100 µM) was applied as a known peroxynitrite scavenger. Samples were subjected to Western blot analysis and stained with an anti ASYN antibody, as well as with an anti 3 nitrotyrosine (3 NT) antibody. Graphs represent the quantitative evaluation of three independent experiments. (**B**) For the identification of nitrated tyrosine residues, a total amount of 10 µg in aliquots of 1 µg of human ASYN was nitrated by authentic PON (5 µM) in the presence and absence of GKT136901 (5 µM). Pooled aliquots were digested by pepsin and subjected to LC MS/MS analysis. Human ASYN contains four tyrosines at the positions 39, 125, 133, and 136.

minutes later, with GKT13690 (PON → GKT136901). In both sets of experiments, the cells were exposed to GKT136901 for about the same time intervals. Uric acid was used in the same experiments as control for a PON scavenger without effect on cell death signaling. Both GKT136901 and the PON-scavenger uric acid protected the cells from PON induced damage when present at the time point of PON addition, but not when given 5 min later (Fig. **7A** & **B**).

4. DISCUSSION

In the present study, we identified the selective scavenging of peroxynitrite (PON) as a novel pharmacological prop-

erty of the NOX-1/4 inhibitor GKT136901. The scavenging properties were first quantified in defined chemical assay systems. Then, the biological relevance of this interaction was illustrated by GKT136901's ability to prevent nitration of alpha synuclein (ASYN), as well as by its protection of human dopaminergic neurons from peroxynitrite (PON) insult. The selectivity of PON scavenging is based on our observation that GKT136901 interacted neither with superoxide ($^{\bullet}O_2^-$) nor nitric oxide ($^{\bullet}NO$), and only moderately with hydroxyl radicals ($^{\bullet}OH$). The selectivity for PON, respectively the $^{\bullet}NO_2$ radical, among other biologically relevant radical species, opens several fields of potential applications of the compound, either independently, or in concert with its inhibitory properties of NOX-1/4.

Similar to previous observations with minocycline or acetaminophen [42, 43], we observed a decomposition of GKT136901 to several products present at low concentrations following PON treatment. The reaction products, originating from the interaction of GKT136901 and PON, did no longer serve as PON scavengers (Fig. **5**). These observations may be relevant for potential clinical applications, as GKT136901 would be typically used under conditions of an inflammatory activation of tissues that is frequently associated with the formation of PON. Our findings suggest that data obtained in experimental models or in clinical studies with drugs such as GKT136901, need to be interpreted with respect to its dual action as NOX-1/4 inhibitor and PON scavenger. In this context, it is important to highlight that PON, although mostly associated with its detrimental effects when formed excessively, serves as cellular regulatory molecule under normal, physiological conditions, e.g. as regulator of prostanoid synthesis by serving as mediator of the so-called peroxide tone, or as regulator of muscle growth [13, 14, 44]. Under conditions of cell activation that are not necessarily associated with cell death conditions, PON plays numerous roles as modulator of cellular signaling cascades. The cysteine-rich zinc-finger motifs in the N-terminal domain of protein kinase C (PKC) for example, are a target for PON-mediated oxidations [45]. PON-dependent activation of PKC can be involved in the phosphorylation and activation of e.g. ERK1/2 or p38, and thereby contribute to cell death [46, 47]. Other prominent examples of PON-mediated regulation are e.g. the nitration of IκBα that results in the activation of NF-κB, or PARP activation by PON-mediated DNA damage [48, 49]. These examples illustrate the significant role of PON as intracellular regulator both under normal, but also under pathophysiological conditions. In a rat diabetic nephropathy model, impaired ERK-1/2 activation by the application of a NOX-1/4 inhibitor was recently detected [30]. This illustrates the necessity to distinguish between the direct NOX inhibitory properties and the PON-scavenging properties of GKT136901, which is indeed complicated by the fact that $^{\bullet}O_2^-$ represents one of PON's adducts.

In the present work, we demonstrated the selective scavenging of PON by the NOX-1/4 inhibitor GKT136901. Contribution of NOX-1 and NOX-4 to oxidative stress conditions have been shown in ischemic injury, in diabetic nephropathy, in hepatocyte apoptosis, or during inflammatory activation of glial cells and even in cortical neurons in the brain [35, 50]. All these pathophysiological conditions are characterized not only by elevated $^{\bullet}O_2^-$ levels, but also by an increased generation of $^{\bullet}NO$, thus allowing the formation of PON [51]. Considering the role of PON as intracellular signaling molecule and its scavenging by low micromolar concentrations of GKT136901, the compound could have the potential to significantly influence inflammation related signaling pathways involved in the execution of cell death.

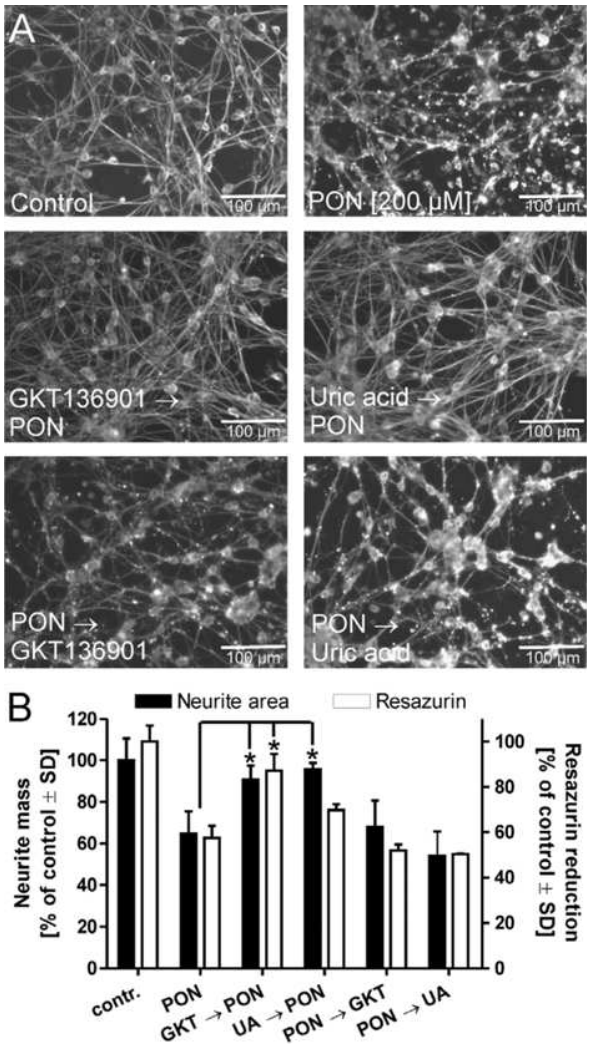

Fig. (7). Protection of dopaminergic neurons by GKT136901. (**A**) Human dopaminergic neurons (LUHMES) in Hanks' balanced salt solution (HBSS) were pre treated with 10 µM GKT136901 or 50 µM uric acid for 5 min and then treated with authentic peroxyni trite (200 µM) (GKT→PON). For comparison, cells were treated with PON first, GKT136901 or uric acid was added after 1 min (PON→GKT). After 5 min, HBSS was replaced by normal LUHMES medium, cells were kept for additional 20 h. The cells were fixed and stained with an anti β III tubulin antibody. Scale bar = 100 µm. (**B**) For quantitative assessment of neurite mass, cells were fixed, stained for β III tubulin and for nuclear DNA (Hoechst H 33342), and analyzed by an automated microscope system. Analysis was performed with an algorithm allowing discrimination between cell bodies and neurites. Cell viability was additionally assessed by the resazurin reduction assay. The data are the means ± S.D. of three independent experiments with four technical replicates respectively. The statistical significance was determined by one way ANOVA, followed by Bonferroni's post hoc test. $^{*}p < 0.05$ versus PON.

CONFLICT OF INTEREST

The authors confirm that this article content has no conflicts of interest.

ACKNOWLEDGEMENTS

We thank Martina Adam for excellent technical assistance. This work was supported by the Collaborative Research Center 969 “Chemical and Biological Principles of Cellular Proteostasis”, funded by the Deutsche Forschungsgemeinschaft (DFG).

ABBREVIATIONS

AAPH	=	2,2-Azobis [2-methyl-propionamidine]
ASYN	=	Alpha synuclein
DHR	=	Dihydrorhodamine
GSH	=	Glutathione
NOS	=	Nitric oxide synthase
NOX	=	NADPH oxidase
PON	=	Peroxynitrite
Sin-1	=	3-morpholino-sydnonimine
SOD	=	Superoxide dismutase
UA	=	Uric Acid

REFERENCES

[1] Bedard, K.; Krause, K.H. The NOX family of ROS-generating NADPH oxidases: physiology and pathophysiology. *Physiol. Rev.*, **2007**, *87*(1), 245-313.

[2] Babior, B.M.; Kipnes, R.S.; Curnutte J.T. Biological defense mechanisms. The production by leukocytes of superoxide, a potential bactericidal agent. *J. Clin. Invest.*, **1973**, *52*(3), 741-744.

[3] Rossi, F.; Zatti, M. Biochemical aspects of phagocytosis in polymorphonuclear leucocytes. NADH and NADPH oxidation by the granules of resting and phagocytizing cells. *Experientia*, **1964**, *20*(1), 21-23.

[4] Suh, Y.A.; Arnold, R.S.; Lassegue, B.; Shi, J.; Xu, X.; Sorescu, D.; Chung, A.B.; Griendling, K.K.; Lambeth, J.D. Cell transformation by the superoxide-generating oxidase Mox1. *Nature*, **1999**, *401*(6748), 79-82.

[5] Cheng, G.; Cao, Z.; Xu, X.; van Meir, E.G.; Lambeth, J.D. Homologs of gp91phox: cloning and tissue expression of Nox3, Nox4, and Nox5. *Gene*, **2001**, *269*(1-2), 131-140.

[6] Babior, B.M.; Lambeth, J.D.; Nauseef, W. The neutrophil NADPH oxidase. *Arch. Biochem. Biophys.*, **2002**, *397*(2), 342-344.

[7] Cross, A.R.; Segal, A.W. The NADPH oxidase of professional phagocytes--prototype of the NOX electron transport chain systems. *Biochim. Biophys. Acta.*, **2004**, *1657*(1), 1-22.

[8] Bánfi, B.; Maturana, A.; Jaconi, S.; Arnaudeau, S.; Laforge, T.; Sinha, B.; Ligeti, E.; Demaurex, N.; Krause, K.H. A mammalian H+ channel generated through alternative splicing of the NADPH oxidase homolog NOH-1. *Science*, **2000**, *287*(5450), 138-142.

[9] Kikuchi, H.; Hikage, M.; Miyashita, H.; Fukumoto, M. NADPH oxidase subunit, gp91(phox) homologue, preferentially expressed in human colon epithelial cells. *Gene*, **2000**, *254*(1-2), 237-243.

[10] Geiszt, M.; Kopp, J.B.; Várnai, P.; Leto T.L. Identification of renox, an NAD(P)H oxidase in kidney. *Proc. Natl. Acad. Sci. U S A.*, **2000**, *97*(14), 8010-8014.

[11] Bánfi, B.; Tirone, F.; Durussel, I.; Knisz, J.; Moskwa, P.; Molnár, G.Z.; Krause, K.H.; Cox, J.A. Mechanism of Ca2+ activation of the NADPH oxidase 5 (NOX5). *J. Biol. Chem.*, **2004**, *279*(18), 18583-18591.

[12] De Deken, X.; Wang, D.; Many, M.C.; Costagliola, S.; Libert, F.; Vassart, G.; Dumont, J.E.; Miot, F. Cloning of two human thyroid cDNAs encoding new members of the NADPH oxidase family. *J. Biol. Chem.*, **2000**, *275*(30), 23227-23233.

[13] Schildknecht, S.; Bachschmid, M.; Ullrich V. Peroxynitrite provides the peroxide tone for PGHS-2-dependent prostacyclin synthesis in vascular smooth muscle cells. *FASEB J.*, **2005**, *19*(9), 1169-1171.

[14] Schildknecht, S.; van der Loo, B.; Weber, K.; Tiefenthaler, K.; Daiber, A.; Bachschmid, M.M. Endogenous peroxynitrite modulates PGHS-1-dependent thromboxane A2 formation and aggregation in human platelets. *Free Radic. Biol. Med.*, **2008**, *45*(4), 512-520.

[15] Mander, P.; Brown, G.C. Activation of microglial NADPH oxidase is synergistic with glial iNOS expression in inducing neuronal death: a dual-key mechanism of inflammatory neurodegeneration. *J. Neuroinflammation.*, **2005**, 2, 20.

[16] Huie, R.E.; Padmaja, S. The reaction of no with superoxide. *Free Radic. Res. Commun.*, **1993**, *18*(4), 195-199.

[17] Beckman, J.S.; Crow, J.P. Pathological implications of nitric oxide, superoxide and peroxynitrite formation. *Biochem. Soc. Trans.*, **1993**, *21*(2), 330-334.

[18] Goldstein, S.; Lind, J.; Merényi, G. Chemistry of peroxynitrites as compared to peroxynitrates. *Chem. Rev.*, **2005**, *105*(6), 2457-2470.

[19] Kissner, R.; Nauser, T.; Bugnon, P.; Lye, P.G.; Koppenol, W.H. Formation and properties of peroxynitrite as studied by laser flash photolysis, high-pressure stopped-flow technique, and pulse radiolysis. *Chem. Res. Toxicol.*, **1997**, *10*(11), 1285-1292.

[20] Aldieri, E.; Riganti, C.; Polimeni, M.; Gazzano, E.; Lussiana, C.; Campia, I.; Ghigo, D. Classical inhibitors of NOX NAD(P)H oxidases are not specific. *Curr. Drug. Metab.*, **2008**, *9*(8), 686-696.

[21] DeLeo, F.R.; Yu, L.; Burritt, J.B.; Loetterle, L.R.; Bond, C.W.; Jesaitis, A.J.; Quinn, M.T. Mapping sites of interaction of p47-phox and flavocytochrome b with random-sequence peptide phage display libraries. *Proc. Natl. Acad. Sci. U.S.A.*, **1995**, *92*(15), 7110-7114.

[22] Williams, H.C.; Griendling, K.K. NADPH oxidase inhibitors: new antihypertensive agents? *J. Cardiovasc. Pharmacol.*, **2007**, *50*(1), 9-16.

[23] Laleu, B.; Gaggini, F.; Orchard, M.; Fioraso-Cartier, L.; Cagnon, L.; Houngninou-Molango, S.; Gradia, A.; Duboux, G.; Merlot, C.; Heitz, F.; Szyndralewiez, C.; Page, P. First in class, potent, and orally bioavailable NADPH oxidase isoform 4 (Nox4) inhibitors for the treatment of idiopathic pulmonary fibrosis. *J. Med. Chem.*, **2010**, *53*(21), 7715-7730.

[24] Ximenes, V.F.; Kanegae, M.P.; Rissato, S.R.; Galhiane, M.S. The oxidation of apocynin catalyzed by myeloperoxidase: proposal for NADPH oxidase inhibition. *Arch. Biochem. Biophys.*, **2007**, *457*(2), 134-141.

[25] Simons, J.M.; Hart, B.A.; Ip Vai Ching, T.R.; Van Dijk, H.; Labadie, R.P. Metabolic activation of natural phenols into selective oxidative burst agonists by activated human neutrophils. *Free. Radic. Biol. Med.*, **1990**, *8*(3), 251-258.

[26] Heumüller, S.; Wind, S.; Barbosa-Sicard, E.; Schmidt, H.H.; Busse, R.; Schröder, K.; Brandes, R.P. Apocynin is not an inhibitor of vascular NADPH oxidases but an antioxidant. *Hypertension*, **2008**, *51*(2), 211-217.

[27] Gaggini, F.; Laleu, B.; Orchard, M.; Fioraso-Cartier, L.; Cagnon, L.; Houngninou-Molango, S.; Gradia, A.; Duboux, G.; Merlot, C.; Heitz, F.; Szyndralewiez, C.; Page, P. Design, synthesis and biological activity of original pyrazolo-pyrido-diazepine, -pyrazine and -oxazine dione derivatives as novel dual Nox4/Nox1 inhibitors. *Bioorg. Med. Chem.*, **2011**, *19*(23), 6989-6999.

[28] Cave, A.C.; Brewer, A.C.; Narayanapanicker, A.; Ray, R.; Grieve, D.J.; Walker, S.; Shah, A.M. NADPH oxidases in cardiovascular health and disease. *Antioxid. Redox. Signal.*, **2006**, *8*(5-6), 691-728.

[29] Garrido-Urbani, S.; Jemelin, S.; Deffert, C.; Carnesecchi, S.; Basset, O.; Szyndralewiez, C.; Heitz, F.; Page, P.; Montet, X.; Michalik, L.; Arbiser, J.; Rüegg, C.; Krause, K.H.; Imhof, B.A. Targeting vascular NADPH oxidase 1 blocks tumor angiogenesis through a PPARα mediated mechanism. *PLoS One*, **2011**, *6*(2), e14665.

[30] Sedeek, M.; Gutsol, A.; Montezano, A.C.; Burger, D.; Nguyen Dinh Cat, A.; Kennedy, C.R.; Burns, K.D.; Cooper, M.E.; Jandeleit-Dahm, K.; Page, P.; Szyndralewiez, C.; Heitz, F.; Hebert, R.L.; Touyz, R.M. Renoprotective effects of a novel Nox1/4 inhibitor in a mouse model of Type 2 diabetes. *Clin. Sci.*, **2013**, *124*(3), 191-202.

[31] Jiang, J.X.; Chen, X.; Serizawa, N.; Szyndralewiez, C.; Page, P.; Schröder, K.; Brandes, R.P.; Devaraj, S.; Török, N.J. Liver fibrosis and hepatocyte apoptosis are attenuated by GKT137831, a novel NOX4/NOX1 inhibitor *in vivo*. *Free. Radic. Biol. Med*., **2012**, *53*(2), 289-296.

[32] Kleinschnitz, C.; Grund, H.; Wingler, K.; Armitage, M.E.; Jones, E.; Mittal, M.; Barit, D.; Schwarz, T.; Geis, C.; Kraft, P.; Barthel, K.; Schuhmann, M.K.; Herrmann, A.M.; Meuth, S.G.; Stoll, G.; Meurer, S.; Schrewe, A.; Becker, L.; Gailus-Durner, V.; Fuchs, H.; Klopstock, T.; de Angelis, M.H.; Jandeleit-Dahm, K.; Shah, A.M.; Weissmann, N.; Schmidt HH. Post-stroke inhibition of induced NADPH oxidase type 4 prevents oxidative stress and neurodegeneration. *PLoS Biol*., **2010**, *8*(9), e1000479.

[33] Choi, S.H.; Aid, S.; Kim, H.W.; Jackson, S.H.; Bosetti F. Inhibition of NADPH oxidase promotes alternative and anti inflammatory microglial activation during neuroinflammation. *J. Neurochem*., **2012**, *120*(2), 292-301.

[34] Wu, D.C.; Ré, D.B.; Nagai, M.; Ischiropoulos, H.; Przedborski, S. The inflammatory NADPH oxidase enzyme modulates motor neuron degeneration in amyotrophic lateral sclerosis mice. *Proc. Natl. Acad. Sci. USA*, **2006**, *103*(32), 12132-12137.

[35] Choi, D.H.; Cristóvão, A.C.; Guhathakurta, S.; Lee, J.; Joh, T.H.; Beal, M.F.; Kim, Y.S. NADPH oxidase 1-mediated oxidative stress leads to dopamine neuron death in Parkinson's disease. *Antioxid. Redox. Signal*., **2012**, *16*(10), 1033-1045.

[36] Cristóvão, A.C.; Choi, D.H.; Baltazar, G.; Beal, M.F.; Kim, Y.S. The role of NADPH oxidase 1-derived reactive oxygen species in paraquat-mediated dopaminergic cell death. *Antioxid. Redox. Signal*., **2009**, *11*(9), 2105-2118.

[37] Schildknecht, S.; Pöltl, D.; Nagel, D.M.; Matt, F.; Scholz, D.; Lotharius, J.; Schmieg, N.; Salvo-Vargas, A.; Leist M. Requirement of a dopaminergic neuronal phenotype for toxicity of low concentrations of 1-methyl-4-phenylpyridinium to human cells. *Toxicol. Appl. Pharmacol*., **2009**, *241*(1), 23-35.

[38] Scholz, D.; Pöltl, D.; Genewsky, A.; Weng, M.; Waldmann, T.; Schildknecht, S.; Leist, M. Rapid, complete and large-scale generation of post-mitotic neurons from the human LUHMES cell line. *J. Neurochem*., **2011**, *119*(5), 957-971.

[39] Stiegler, N.V.; Krug, A.K.; Matt, F.; Leist, M. Assessment of chemical-induced impairment of human neurite outgrowth by multiparametric live cell imaging in high-density cultures. *Toxicol. Sci*., **2011**, *121*(1), 73-87.

[40] Schildknecht, S.; Gerding, H.R.; Karreman, C.; Drescher, M.; Lashuel, H.A.; Outeiro, T.F.; Di Monte, D.A.; Leist, M. Oxidative and nitrative alpha-synuclein modifications and proteostatic stress: implications for disease mechanisms and interventions in synucleinopathies. *J. Neurochem*., **2013**, *25*(4), 491-511.

[41] Robinson, K.M.; Morré, J.T.; Beckman, J.S. Triuret: a novel product of peroxynitrite-mediated oxidation of urate. *Arch. Biochem. Biophys*., **2004**, *423*(1), 213-217.

[42] Schildknecht, S.; Pape, R.; Müller, N.; Robotta, M.; Marquardt, A.; Bürkle, A.; Drescher, M.; Leist, M. Neuroprotection by minocycline caused by direct and specific scavenging of peroxynitrite. *J. Biol. Chem*., **2011**, *286*(7), 4991-5002.

[43] Schildknecht, S.; Daiber, A.; Ghisla, S.; Cohen, R.A.; Bachschmid, M.M. Acetaminophen inhibits prostanoid synthesis by scavenging the PGHS-activator peroxynitrite. *FASEB J*., **2008**, *22*(1), 215-224.

[44] Ito, N.; Ruegg, U.T.; Kudo, A.; Miyagoe-Suzuki, Y.; Takeda, S. Activation of calcium signaling through Trpv1 by nNOS and peroxynitrite as a key trigger of skeletal muscle hypertrophy. *Nat. Med*., **2013**, *19*(1), 101-106.

[45] Li, S; Lin, W.; Tchantchou, F.; Lai, R.; Wen, J.; Zhang Y. Protein kinase C mediates peroxynitrite toxicity to oligodendrocytes. *Mol. Cell. Neurosci*., **2011**, *48*(1), 62-71.

[46] Bapat, S.; Verkleij, A.; Post, J.A. Peroxynitrite activates mitogen-activated protein kinase (MAPK) via a MEK-independent pathway: a role for protein kinase C. *FEBS Lett*., **2001**, *499*(1-2), 21-26.

[47] Jope, R.S.; Zhang, L.; Song, L. Peroxynitrite modulates the activation of p38 and extracellular regulated kinases in PC12 cells. *Arch. Biochem. Biophys*., **2000**, *376*(2), 365-370.

[48] Yakovlev, V.A.; Barani, I.J.; Rabender, C.S.; Black, S.M.; Leach, J.K.; Graves, P.R.; Kellogg, G.E.; Mikkelsen, R.B. Tyrosine nitration of IkappaBalpha: a novel mechanism for NF-kappaB activation. *Biochemistry*, **2007**, *46*(42), 11671-1183.

[49] Pacher, P.; Szabo, C. Role of the peroxynitrite-poly(ADP-ribose) polymerase pathway in human disease. *Am. J. Pathol*., **2008**, *173*(1), 2-13.

[50] Vallet, P.; Charnay, Y.; Steger, K.; Ogier-Denis, E.; Kovari, E.; Herrmann, F.; Michel, J.P.; Szanto, I. Neuronal expression of the NADPH oxidase NOX4, and its regulation in mouse experimental brain ischemia. *Neuroscience*, **2005**, *132*(2), 233-238.

[51] Bal-Price, A.; Matthias, A.; Brown, G.C. Stimulation of the NADPH oxidase in activated rat microglia removes nitric oxide but induces peroxynitrite production. *J. Neurochem*., **2002**, *80*(1), 73-80.